

The final publication is available at <http://link.springer.com>.

Supplementary Material

ICAT: A Computational Model for the Adaptive Control of Fixation Durations

Hans A. Trukenbrod, Ralf Engbert
University of Potsdam

This Supplementary Material is part of an article published at *Psychonomic Bulletin & Review* (<http://dx.doi.org/10.3758/s13423-013-0575-0>).

Corresponding Author:

Hans A. Trukenbrod
Universität Potsdam
EB Kognitionswissenschaften
Karl-Liebknecht-Str. 24-25
14476 Potsdam
Germany

E-Mail: Hans.Trukenbrod@uni-potsdam.de

Phone: +49 (0)331 977-2874

Fax: +49 (0)331 977-2793

Contents

Introduction to the Supplementary Material	3
ICAT: Simulations of immediacy effects and distributions of saccade initiation times	4
A model of eye guidance during scanning	9
Dynamic field of activations	9
Processing rate and visual acuity	9
Temporal evolution of activations	10
Target selection	11
Saccade programming	11
Stochastic simulation of saccade programming and execution	12
Model overview	16
Specific model assumptions for the scanning task	16
Estimation of model parameters for the full eye movement model	19
Simulation studies: Target selection & oculomotor control	23
Experiment 1: Stepwise processing change during visual search	23
Experiment 2: Gaze-contingent display presentation	25
Experimental Details	30
Experiment 1: Stepwise change in processing demands	30
Experiment 2: Gaze contingent display presentation	31
References	31

Introduction to the Supplementary Material

The main text focussed on the temporal control of fixation durations, in general, and the interaction of global and local control principles, in particular. Therefore, a number of details were only mentioned briefly. In order to make our modeling as transparent as possible, we decided to provide this information as Supplementary Material. The first section demonstrates that the simple version of ICAT (without spatial control) is able to generate immediacy effects in mean fixation durations as well as corresponding fixation duration distributions. Simulations revealed that ICAT even reproduces multimodal fixation duration distributions. The second section describes how ICAT can be equipped with a set of spatial control principles as well as details about parameter estimation. The third section summarizes the results related to the spatial control principles of the full model: a) Probabilities of different saccade types and b) oculomotor phenomena related to the fixation position within a symbol. Finally, the fourth section provides details of our experimental setup.

ICAT: Simulations of immediacy effects and distributions of saccade initiation times

Immediacy effects, i.e., influences of the fixated region on fixation durations, are a first important benchmark for models describing the control of fixation durations. Since ICAT approximates fixation duration distributions we can even compare the model’s performance with experimentally observed fixation duration distributions. In a first step, we apply our model to an experiment by Yang and McConkie (2001), which was one of the major motivations for the ICAT architecture. In a second step, we investigate two reading experiments reported by Staub, White, Drieghe, Hollway, and Rayner (2010). The experiments showed an early influence of frequency on fixation durations and let the authors conclude that saccades are initiated by lexical processing, i.e., a cognitive trigger. In addition, we compare our model to results from a gaze-contingent manipulation by Reingold, Reichle, Glaholt, and Sheridan (2012). Finally, we investigate the influence of word predictability on saccade timing (Staub, 2011).

The first experiment (Yang & McConkie, 2001) examined adjustments of fixation durations in a gaze-contingent paradigm. Fixation durations during normal reading were compared with fixations when the page was replaced by (i) a stimulus visually similar to the original text or (ii) a stimulus visually strongly deviating from the original text.¹ Fixation duration distributions during normal reading showed a pronounced peak (Fig. 1c). When the stimulus was replaced by a similar stimulus, saccades after long fixation durations (> 275 ms) were executed with a delay (Fig. 1d). In contrast, strong visual manipulations disrupted the execution of saccades already shortly after fixation onset (175 – 225 ms) resulting in a bimodal distribution (Fig. 1e). In all conditions fixation durations below 150 ms were unaffected by stimulus properties.

For model simulations we used a fixed set of parameters (see Table 1) and assumed that experimental conditions differed in terms of processing (Fig. 1a). During normal reading activations rise to a moderate level and return soon to zero. When words are replaced by a similar stimulus, activations rise at a similar rate and processing difficulties lead to late increased activations. Only strong visual perturbations affect processing rates immediately and produce early high activations. Rate modulations are shown in (Fig. 1b). Saccade timing is adjusted to normal reading (solid line). Transition rates are only weakly modulated by low activations, but are strongly affected by activations exceeding this maximum. Parameters as well as the different time-courses of activations were chosen by visual inspection of the resulting distributions.² In general, shapes of the experimental and simulated distributions are very similar. Both early and late modulations can be observed with a single set of saccade timing parameters.

Since display changes occurred rarely and were apparent to the reader in the study

¹In the original work Yang and McConkie (2001) tested seven different conditions. We extracted data points from Figure 2 and subsequently averaged across similar conditions. The first distribution contained normal reading only (normal+), the second distribution three conditions with a stimulus visually similar to the original stimulus (normal-, nonword+, X’s+), and the third distribution the remaining conditions (X’s-,dash+,blank-).

²In this section we did not use a computational optimization technique since we wanted to qualitatively demonstrate the models viability. Even though we did not aim for the best fit, the quantitative fits are in good agreement with the experimental data.

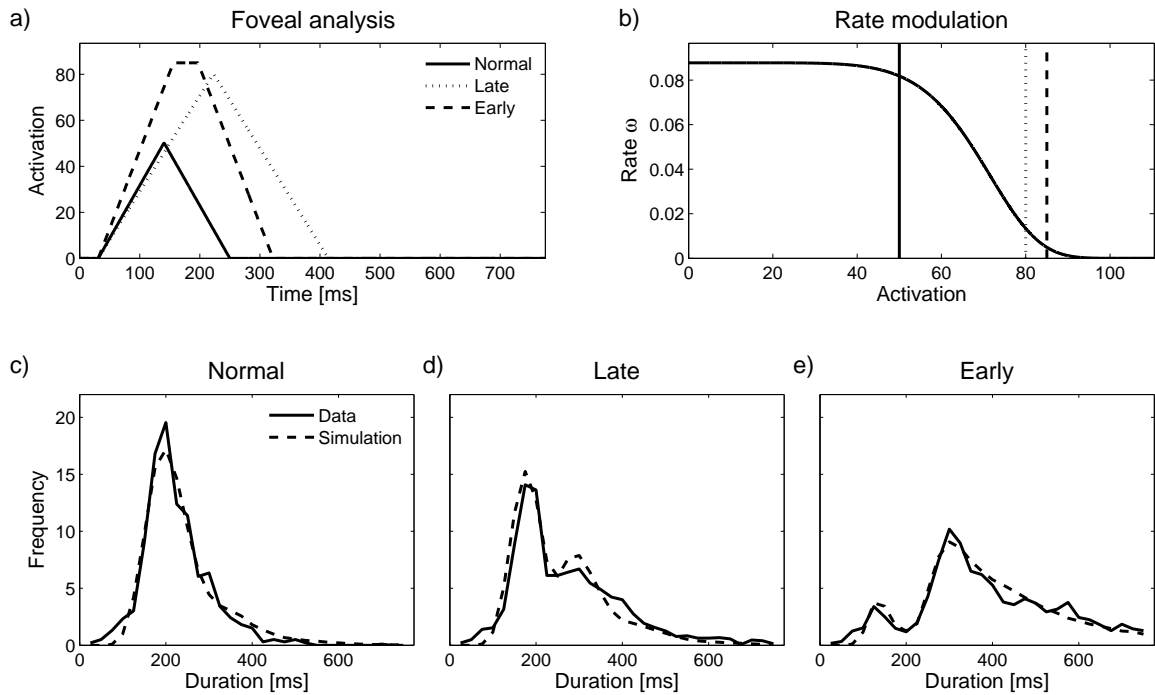


Figure 1. Simulation results of Yang and McConkie's (2001) fixation duration distributions. a) Temporal evolution of activations used in simulations. b) Foveal inhibition. Maximal activations of each condition are marked as vertical lines. Saccade timing is adapted to normal reading. c-e) Simulation results during normal reading, late and early disruptions of the fixation. Experimental data points correspond to fixation durations, simulated data points to saccade initiation times.

by Yang and McConkie (2001), the paradigm might be an unusual situation that does not generalize to tasks like normal reading (Rayner, Pollatsek, & Reichle, 2003). Rayner, Yang, Castelano, and Liversedge (2011) confirmed this notion by showing that rare and quasi-randomly placed display changes generate more disruption to fixations compared to masking every word. In order to test whether our model accounts for less artificial eye-movement data we used reanalyses of fixation duration distributions (Staub et al., 2010) applied to two reading experiments manipulating word-frequency (Drieghe, Rayner, & Pollatsek, 2008; White, 2008). Word frequency has two major effects on fixation duration distributions. First, low-frequency words shift the entire distribution towards longer durations. Second, low-frequency words affect the skewness of a distribution resulting in a larger frequency effect for long fixation durations.

Model simulations are depicted in Figure 2 (upper panels: Drieghe et al., 2008; lower panels: White, 2008). Activations of low-frequency words generate a higher maximum and processing time is prolonged (Fig. 2a). The corresponding rate modulations are plotted in Figure 2b. The chosen parameter combination (Table 1) generates an asymmetric control of fixation durations, since activations below the adjusted difficulty (solid vertical line) do not affect rate while higher activations generate a sharp decline. Resulting vincentile plots of

Table 1: Model parameters for simulation 1-4. Values in parentheses represent parameters modified for simulation of different conditions. For these simulations primarily parameters related to visual processing were varied. Some of the variability can be attributed to large differences between tasks. All parameters were hand-tuned to demonstrate qualitatively the broad range of behaviors that can be generated by the ICAT principles.

Parameter	Symbol	Yang & McConkie (2001)	Drieghe (2008)	White (2008)	Staub (2011)	Eq. in main text
Processing activations						
Maximum	A_j	50.0 (80.0/85.0)	50.0 (65.0)	50.0 (65.5)	50.0	5 & 8
Rise		0.46 (0.42/0.68)	0.93	0.93	0.93	
Plateau		0.0 (0.0/40.0)	0.0	0.0	0.0	
Onset		30.0	0.0	0.0	0.0	
Saccade timer						
Timer states	N_t	18	18	18	19 (17/21)	3
Duration ^a	T_j	205	245	240	195 (212)	3 & 7
Foveal inhibition	α	0.07	0.075	0.075	0.075	5
	β	7.0	12.0	12.0	12.0	5
Saccade programming						
Oculomotor states	N_o	20.0	20.0	20.0	20.0	11
Duration ^a (labile)	τ_{lab}	150.0	150.0	135.0	125.0	11

^aAll durations are presented in ms.

experimental fixation durations (lines) and simulated data (markers) are in good agreement (Fig. 2c). Data points in vincentile plots correspond to mean fixation durations representing the shortest 10% of fixation durations, the next 10%, and so on. The two effects of word frequency (i.e., a shift of the entire distribution and a larger frequency effect for long fixation durations) are best illustrated by looking at the difference between mean fixation durations of low- and high-frequency words for each data point (Fig. 2d). Even though saccades are not triggered by lexical processing in our model, the influence of lexical processing on foveal inhibition is sufficient to affect the entire range of fixation durations as well as generating larger frequency effects for longer fixation durations. Reingold et al. (2012) replicated the effects on both shift and skewness. In addition, preventing preview of target words before fixation and thus delaying visual processing of words, reduced the number of fixations affected by frequency from about 90% to about 40%. Furthermore, the shift of the distribution for low-frequency words disappeared, while the skewness remained unaffected. Following Reingold et al. (2012), we fitted ex-Gaussian distributions to first-fixation durations generated in our simulations. By delaying the temporal evolution of activations by 150 ms, the shift in fitted ex-Gaussian distributions vanished while the skewness remained. Both experiment and simulation showed no effect on the variance parameter.

Finally, we investigated the influence of word predicability on saccade timing within the ICAT model. Using the same analyses as in the previous paragraph, Staub (2011)

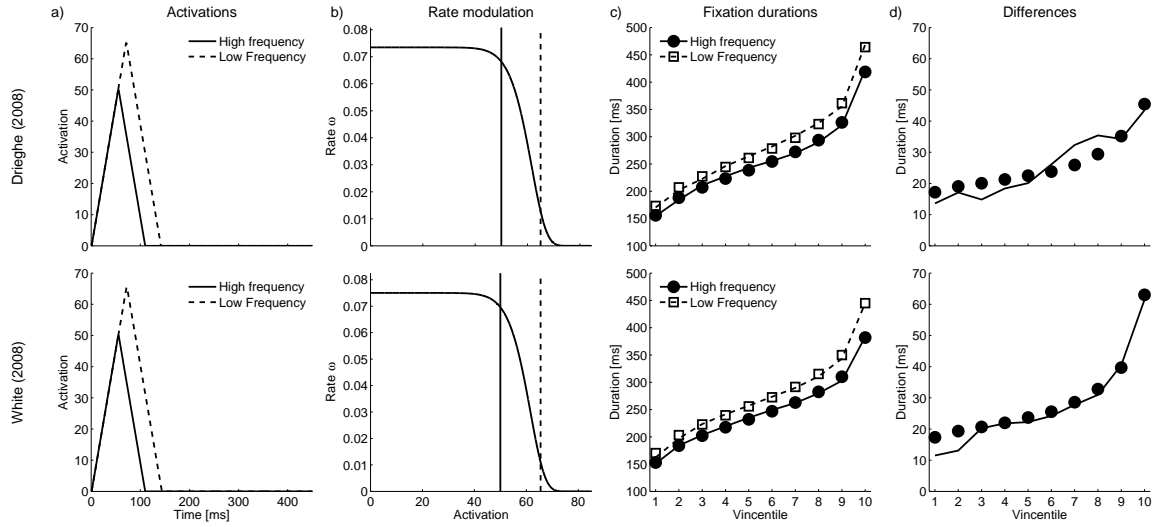


Figure 2. Simulation of frequency effects on first-fixation durations (FFD) during reading studied by Drieghe et al. (2008; upper panels) and White (2008; lower panels). a) Temporal evolution of activations for high- and low-frequency words. b) Rate modulation through foveal inhibition. c) Vincentile plots of FFDs. d) Difference in mean FFD between high- and low-frequency words at different vincentiles. Data taken from Staub et al. (2010).

demonstrated that low predictable words shift the distribution of fixation durations, while leaving skewness and variance of fitted ex-Gaussians unaffected. In our simulations, we assumed that the mean timer duration T_j as well as the number of states N_t depended on word predictability. The resulting foveal inhibition functions are shown in Figure 3b. In both cases activations for high and low predictable words remain below the expected difficulty, since expected difficulty should on average be well adapted (vertical line). Distributions of first-fixation durations as well as the predictability effect are shown for both experiment (lines) and simulations (markers) in Figure 3c-d. The model was able to reproduce the observed pattern by assuming different saccade timing parameters prior to fixating a high or low predictable word. Saccade timing was affected by adjusting (i) the expected duration of the next fixation (see Eq. 8 in the main text) and (ii) the number of states N_t , which alters the variance generated by random walks. Even though visual inspection of the experiment suggests a slight effect on skewness, which could be captured by our model (solid line and filled dots in Fig. 3d), Reingold et al. (2012) observed no effect in the fitted ex-Gaussian distributions. The visual effect was most likely generated by a few outliers. Therefore, we investigated whether the model is able to generate a pure shift of the distribution. In a second simulation, we kept the estimated parameters and changed only the number of states N_t from 17 to 21. With these parameters a flat line is observed (open circles). Simulations of predictability indicate that saccade timing is affected before fixating the corresponding word. Interestingly, we were not able to reproduce the effect by changing other parameters and keeping saccade timing parameters constant. Hence, predictability (a contextual

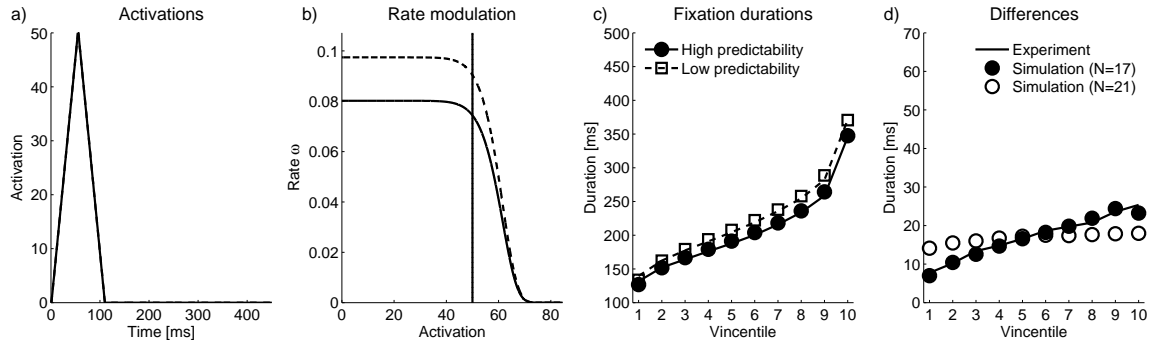


Figure 3. Simulation of predicability effects on first-fixation durations (FFD) during reading. a) Temporal evolution of activations for high- and low-predictable words. b) Rate modulation through foveal inhibition. c) Vincentile plots of FFDs. d) Difference in mean FFD between high- and low-predictable words at different Vincentiles. Filled dots correspond to simulations in panel a-c. Open dots show the result of a simulation with no effect on skew. Data taken from Staub et al. (2011).

constraint) has a major influence on saccade timing even before fixating the corresponding word.

In summary, the ICAT model is able to replicate a number of fixation duration distributions in reading and reading-like tasks. Even strong disturbances of fixation duration distributions as generated by rare display changes can be reproduced by our model. Furthermore, the frequency effects and specific modulations of the corresponding distributions are captured by the model. Interestingly, frequency effects have been interpreted as evidence for control by cognitive triggers, since the entire range of fixation durations is affected (Rayner, Liversedge, White, & Vergilino-Perez, 2003; Reingold, Yang, & Rayner, 2010; Staub et al., 2010). We showed that an autonomous saccade timer with inhibitory control is able to generate the observed fixation duration patterns including a stronger frequency effect on long fixations and an effect on skewness but no shift in the distribution when visual input is delayed. Finally, saccade timer adjustments seem to be affected not only by fixation history but also by expectations of upcoming words.

A model of eye guidance during scanning

After introducing the general principles of fixation duration control of the ICAT model in the main manuscript, we now discuss how the model may be combined with assumptions about spatial control. While it is possible to use ICAT's saccade timing within a serial attention shift model of spatial control of eye movements, we argued earlier (Engbert & Kliegl, 2011) that indirect control principles of fixation durations are more naturally combined with a dynamic field theory (Amari, 1977; Erlhagen & Schöner, 2002). As an example for a dynamic field theory for eye-movement control in reading, we proposed the SWIFT model for the generation of saccades during reading (Engbert, Nuthmann, Richter, & Kliegl, 2005).

Dynamic field of activations

In SWIFT, a single set of activations $\{a_n(t)\}$ is used to keep track of lexical processing of word $n = 1, 2, 3, \dots, N$ and for target selection. As a result, all types of saccades observed in reading experiments are predicted by the set of distributed activations. In the following, we assume that a discrete set of items is available, so that a unique mapping between items and activations exists. For the numerical simulations we use a scanning task with a horizontal row of stimuli. This simplification is not a fundamental limitation of the modeling approach (the dynamic field theory of movement planning is continuous in both time and space). For more complex visual search tasks or scene viewing, the set of activations can be extended to a continuous two-dimensional field.

The set of activations $\{a_n(t)\}$ is shaped by processing and can be interpreted as a (dynamical) saliency map (Koch & Ullman, 1985) which is used for the selection of saccade targets. Temporal evolution of each activation $a_n(t)$ is divided into two stages. During a first stage, activation $a_n(t)$ increases and, consequently, the probability of selecting object n as the next saccade target increases (i.e., it becomes more and more salient). After reaching a maximum value, A_n , activations decrease, until they return to a minimum of $a_n(t) = 0$. Here we consider the case that a stimulus or object n is completely processed when the minimum activation is reached. However, in tasks with recurrent visits of a particular region (e.g., scene viewing), a natural extension of our model would be to permit multiple processing cycles after a first fixation within the region of object n .

The rise and decline of activations serve two major purposes in our model. First, activations reflect processing progress. We assume that low level properties like symbol location become available before higher level properties like item identity. A clear cut distinction of these processes, however, is not intended by the temporal evolution of activations. Second, activations represent potential saccade targets. In order to allow for forward movements, refixations, and regressions activations need to evolve rather slowly over time.

Processing rate and visual acuity

Activation-field dynamics are based on distributed processing (Engbert, Longtin, & Kliegl, 2002; Engbert & Kliegl, 2011). As one of the landmark findings in the 1970s, the perceptual span has been explored in detail in reading (McConkie & Rayner, 1975; Rayner, 1975; Rayner & Bertera, 1979). Here we use the operational definition of *processing span* as the area around the fixation location from which information is extracted for the control

of eye movements. At least three factors contribute to the shape of the processing span: Visual acuity, crowding, and task-dependent attention allocation. It is important to note that for particular aspects of information extraction, different (and more rigorously defined) notions of processing spans are proposed, however, the model developed here aims at a very general concept of processing, not addressing the details of particular tasks.

In our model, visual acuity and crowding are a function of the distance from the center of the visual field. The horizontal distance (or eccentricity) ε_n of a stimulus n to the fixation position is given by

$$\varepsilon_n(t) = \chi_n - k(t) , \quad (1)$$

where χ_n represents the center of stimulus element n and $k(t)$ the absolute fixation position³ at time t .

In addition, the perceptual span is asymmetrical during reading (McConkie & Rayner, 1976; Pollatsek, Bolozky, Well, & Rayner, 1981) and is expected to be asymmetrical in left-to-right scanning tasks as well. Following Engbert et al. (2005), we approximate the spatial properties of the processing span by an asymmetric Gaussian function to capture the relation between processing rate and visual eccentricity. The maximum processing rate is found at the center of fixations and decreases monotonically with increasing eccentricity. Due to the asymmetric span, processing rate declines steeper to the left than to the right. Mathematically, processing rate $\lambda_n(t)$ of stimulus element n at time t is computed by

$$\lambda_n(t) = \lambda_0 \exp \left(-\frac{\varepsilon_n^2(t)}{2\sigma^2} \right) \text{ with } \begin{cases} \sigma = \sigma_L, & \text{if } \varepsilon_n(t) < 0 \\ \sigma = \sigma_R, & \text{if } \varepsilon_n(t) \geq 0 \end{cases} , \quad (2)$$

where the width of the processing span is characterized by σ_L (extension to the left) and σ_R (extension to the right). The parameter λ_0 is a normalization constant, so that processing rate over the total span sums to one. Hence, λ_0 is a function of σ_L and σ_R ,

$$\lambda_0 = \sqrt{\frac{2}{\pi}} \frac{1}{\sigma_L + \sigma_R} , \quad (3)$$

and is not a free parameter in our model.

Temporal evolution of activations

Before preprocessing a stimulus is unknown, after processing the object is identified. In both cases activations will have a value of zero and will not attract the eyes as possible saccade targets. As noted above, the uni-modal relation between activation and processing can be relaxed to multiple processing cycles for specific tasks. Since Following Engbert et al. (2002, 2005), the temporal evolution of activations is controlled by a system of N coupled ordinary differential equations,

$$\frac{da_n(t)}{dt} = f_n(t)\lambda_n(t) - \kappa , \quad (4)$$

where (i) $f_n(t)$ is a factor representing the two processing stages with increasing and decreasing activation, (ii) $\lambda_n(t)$ is the processing rate of stimulus element n , and (iii) κ gives

³In a two-dimensional version, the scalar quantities $k(t)$, χ_n , and $\varepsilon_n(t)$ would be vector-valued variables $\vec{k}(t)$, $\vec{\chi}_n$, and $\vec{\varepsilon}_n(t)$, respectively.

the strength of a global decay process. The decay process induces a slow (compared to processing speed in foveal vision) decrease at a constant rate across the entire activation field and is motivated by memory leakage. During preprocessing, $f_n(t) = f$, activation $a_n(t)$ of symbol n rises to its maximum value A_n , which is interpreted as the processing difficulty. In a second processing stage, $f_n(t) = -1$, activation $a_n(t)$ declines to zero.

Target selection

In our model, processing over time is reflected in a set of activations $\{a_n(t)\}$. One of the major advantages of this field-theoretic approach (Erlhagen & Schöner, 2002; Engbert et al., 2002) is that relative activations determine target-selection probabilities. Except for specification of some details for the computation of probabilities from the set $\{a_n(t)\}$ at time t , no additional assumptions are necessary. Here we implement target selection, by considering all stimulus elements n with some non-vanishing activation, $a_n(t) > 0$. Mathematically the probability $\pi_n(t)$ of selecting a stimulus element n as a saccade target at time t is given by its relative activation,

$$\pi_n(t) = \frac{a_n^\gamma(t)}{\sum_{j=1}^N a_j^\gamma(t)} \quad \text{with} \quad \sum_{n=1}^N \pi_n(t) = 1, \quad (5)$$

where N is the number of target objects and the exponent γ is a measure of stochasticity in the target selection process. Two extreme forms of target selection can be distinguished. For $\gamma \rightarrow \infty$ target selection is a deterministic process, where the highest activation is chosen as the next saccade target (“winner-takes-all”). In contrast, for $\gamma = 0$ all activated symbols have the same probability to be chosen as the target during the next saccade (random target selection). In our simulations, this parameter is set to a value of $\gamma = 0.1$ (see also Engbert & Kliegl, 2011).

Saccade programming

As mentioned earlier, preparation of saccades is a two-stage process with a labile and a non-labile programming stage (Becker & Jürgens, 1979). After initiation of a new saccade program in the ICAT model, a labile stage with mean duration T_{lab} starts. If a second saccade program is initiated during this stage, the labile saccade program will be canceled and replaced by a new labile saccade program. After termination of the labile stage, a non-labile stage with average duration T_{nlab} is entered. If a new labile saccade program is initiated while the non-labile stage is active, two saccade programs will be programmed in parallel resulting in reduced fixation durations during the next fixation (McPeck, Skavenski, & Nakayama, 2000).⁴ Saccade targets after short saccade latencies are based on information accumulated during the previous fixation (Caspi, Beutter, & Eckstein, 2004) and both coding and maintenance of a second saccade target before initiation of the first saccade has been reported for neurons in the superior colliculus (McPeck & Keller, 2002). The transition from a labile to non-labile programming stage triggers the selection

⁴Percent of concurrent saccade programs was estimated by numerical simulations for Experiment 1 (10.5%) and Experiment 2 (2.5%). The huge difference between both simulations results from the differences in saccade timing. Parallel programming of saccades is much more likely if saccades are initiated after short time intervals.

Table 2: Transition events and transition rate.

Random walk	Transition from $S_m = (m_1, m_2, m_3, m_4)$ to $S_n = \dots$				Transition rate
Saccade timer ^a	$m_1 + 1$	m_2	nl	ex	$\omega_j(t)$
Labile program ^a	m_1	$m_2 + 1$	nl	ex	$\omega_{lab}(t)$
Non-labile program ^a	m_1	m_2	$nl + 1$	ex	$\omega_{nlab}(t)$
Saccade execution ^a	m_1	m_2	nl	$ex + 1$	$\omega_{ex}(t)$

^aAfter exceeding a threshold random walks are reset to zero.

of the next saccade target (see Eq. (5)). After termination of a non-labile saccade program, a saccade is executed with mean duration T_{ex} . Since *saccadic suppression* strongly reduces visual input during saccades (Matin, 1974), preprocessing is interrupted immediately after the execution of a saccade for 50 ms. The temporal delay of this interruption is in accordance with the eye-brain lag (Foxy & Simpson, 2002; Lamme & Roelfsema, 2000). In the second processing stage, symbol identification is unaffected by saccadic suppression, since visual input is more critical for early processing.

Stochastic simulation of saccade programming and execution

In the section on saccade timing, we introduced stochastic simulation of multiple random walks within a coherent framework (Gillespie, 1978). Here, we extend this framework to four Markov processes in order to implement all levels of saccade control, i.e., saccade initiation, labile and non-labile saccade programs, and saccade execution. In this case, the dynamical state of the model is defined by a vector $S_m = (m_1, m_2, m_3, m_4)$, where $m_1 = 0, 1, 2, \dots, N_t$ is the state of saccade timing, m_2 is related to the labile saccade program, m_3 represents the non-labile program, and m_4 denotes the state of saccade execution. Accordingly, there are four possible transitions from state S_m to the adjoined states S_n (Table 2).

Since saccade timing, saccade programming, and saccade execution consist of four independent one-step processes, total transition probability $W_m(t)$ at time t is given by (cf., Eq. (9) in main text),

$$W_m(t) = w_j(t) + w_{lab}(t) + w_{nlab}(t) + w_{ex}(t) \quad (6)$$

where $w_j(t)$ is the time-dependent transition probability of the random walk implemented in the ICAT model of saccade timing (cf., Eq. (6) in main text) and the transition probabilities w_{lab} , w_{nlab} , and w_{ex} correspond to the transition probabilities of the labile/non-labile saccade programs and saccade execution. Calculation of the waiting time τ as well as the corresponding transition probabilities $p_n(t)$ can be done by using Equations (2) and (12) in the main text.

While the transition rate $w_j(t)$ of the saccade timer is always non-zero, random walks of the oculomotor system are only active, when the corresponding saccadic process has been initiated. For example, the labile program starts when the random walk of the saccade timer reaches the threshold and terminates when reaching its own threshold while simultaneously triggering the non-labile stage. After entering a stage of saccade programming or during

the execution of a saccade, rates of corresponding random walks are given by

$$\begin{aligned}
 w_{lab}(t) &= \frac{N_o}{T_{lab}} h_j[a_f(t)] && \text{during labile stage} \\
 w_{nlab}(t) &= \frac{N_o}{T_{nlab}} && \text{during non-labile stage} \quad , \\
 w_{ex}(t) &= \frac{N_o}{T_{ex}} && \text{during saccade execution}
 \end{aligned} \tag{7}$$

where N_o is the number of states of oculomotor random walks, T_{lab} , T_{nlab} , and T_{ex} denote the average duration of the respective process, and $h_j[a_f(t)]$ is the strength of foveal inhibition (see Eq. (5) in main text). Since foveal inhibition ranges between 0 to 1, transition rates of labile saccade programs may be reduced by foveal inhibition.

The interplay of all random walks during a trial is illustrated in Figure 4a. Figure 4b is an enlarged view of the gray part of Figure 4a. The random walk of the autonomous saccade timer is shown at the bottom. Random walks of the labile and non-labile saccade programming stages are shown in the central rows, and the random walk of the executed saccade is plotted at the top. The random walk of the saccade timer is continuously active and rises towards the predefined threshold N_t . When reaching this threshold a cascade of events begins. First, the random walk is reset to zero; second, a labile saccade program is initiated. Now, two random walks evolve simultaneously over time with different mean durations and thresholds (active random walks are plotted with black lines). At the end of the labile saccade program, the corresponding random walk is inactivated and set to zero and the target of the next saccade is chosen. At the same time, the random walk of the non-labile program starts. Likewise, this random walk is reset and inactivated at the end of the non-labile saccade program and triggers the random walk of the executed saccade. After saccade execution, all but the random walk of the saccade timer are inactive until it reaches the threshold anew.

A timeline of events is shown in Figure 4c. The upper column shows the sequence of saccade programs. Until a labile saccade program is initiated, the saccadic system remains in a decision mode (D) where only the saccade timer is active. Subsequently a labile (L) and non-labile saccade program (N) is executed, followed by the executed saccade (S). Fixations (F) comprise the time between two saccades which consist of three different parts: A decision period, the duration of a labile saccade program, and the duration of a non-labile saccade program. Variability of fixation durations is generated at two independent levels: Saccade initiation and saccade programming. Variability on the level of saccade initiation affects the decision period, while variability on the level of saccade programming affects durations of the labile and non-labile stages.

According to the stochastic simulation framework, multiple random walks can be active simultaneously. Constraints imposed by values of the estimated parameters and by the architecture of the model, however, hamper the execution of multiple random walks. For our subsequent simulations we estimated the percentage of time with a single active random walk (Experiment 1 $\approx 15.75\%$; Experiment 2 $\approx 35.72\%$), two random walks active in parallel (82.26%; 64.00%), and three or more active processes (1.99%; 0.27%).⁵

⁵In the case of three active random walks, two different saccades are programmed simultaneously: As soon as the non-labile programming stage is entered, a new labile saccade program may be initiated.

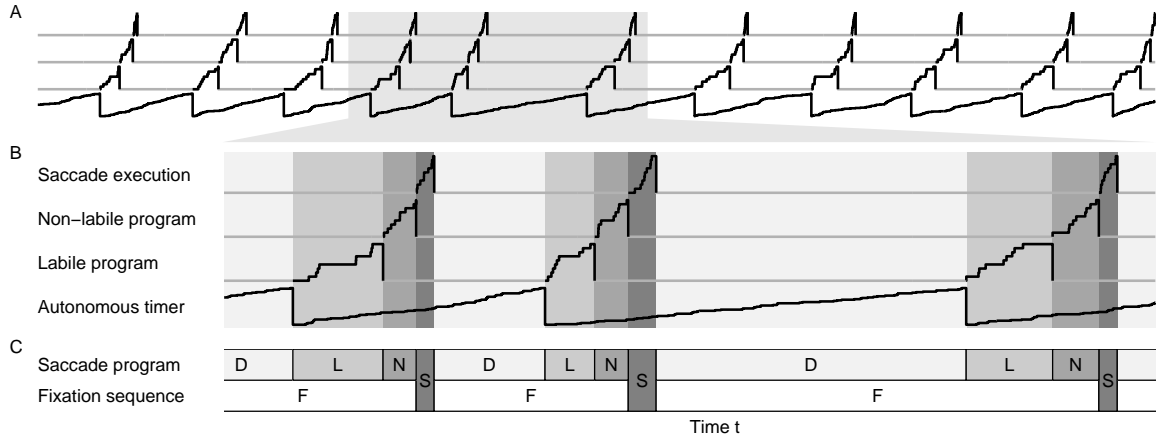


Figure 4. Parallel simulation of random walks for sub-processes. (a) Simulation of a single trial. (b) Magnification of highlighted area. In the model random walks determine stochasticity at four different levels: The timer initiating new saccade programs, labile and non-labile saccade programs, as well as the executed saccades. Periods with active random walks, i.e., $\omega > 0$, are plotted as black lines; inactive random walks, i.e., $\omega = 0$, are plotted as gray lines. (c) Sequence of events at the saccadic level (saccade program) and observable behavioral level (fixation sequence). Fixations (F) are the time between two saccades (S) and consist of a decision period (D), a labile saccade program (L), and a non-labile saccade program (N).

Oculomotor errors in saccade generation. Assumptions about saccadic errors in SWIFT (Engbert et al., 2005) are based on results by McConkie, Kerr, Reddix, and Zola (1988). During reading, saccades are directed toward the center of a word, but are modulated by a systematic and a random error component, so that the observed mean fixation position is typically characterized by a small deviation from the word center. Both error components can be observed in simple oculomotor tasks (Kapoula, 1985) as well as visual search tasks (Trukenbrod & Engbert, 2007). Across tasks both components contribute differently to the observed saccade amplitudes. Recent results demonstrated that such stochastic variation of landing position can be explained by Bayesian estimation in the case of text reading (Engbert & Krügel, 2010), which might offer a more parsimonious implementation of oculomotor errors for future modeling work.

The realized saccade length l consists of three linearly combined components (McConkie et al., 1988), i.e.,

$$l = l_I + l_{SRE} + l_G. \quad (8)$$

The intended saccade amplitude l_I is the distance to the *optimal viewing position* of the next target (McConkie, Kerr, Reddix, Zola, & Jacobs, 1989), which is modified by a systematic error component l_{SRE} and by random noise l_G in the oculomotor system. In our simulations the intended saccade amplitude is the distance of the fixation position to the center of the next saccade target.

The systematic error component is known as *range error* (Kapoula, 1985; Poulton, 1981), which produces a systematic deviation from the intended saccade amplitude l_I to-

wards a preferred saccade length l_0 . The deviation is proportional to the difference between intended and preferred saccade length,

$$l_{sre} = \delta_{SRE} (l_0 - |l_I|), \quad (9)$$

with a factor δ_{SRE} regulating the strength of the saccadic range error. Because of this systematic error component, saccades tend to overshoot the target when the target is closer to the launch site than the preferred saccade length, $l_0 > l_I$, and tend to undershoot the target when it is farther away, $l_0 < l_I$.

In addition, saccade amplitudes are altered by a random error component. The random error is implemented as Gaussian noise with zero mean and standard deviation σ_G . Variance of random errors increases with movement amplitude in almost all motor control processes (Poulton, 1981). For simplicity, we assume a linear relation between standard deviation σ_G and intended saccade amplitude l_I with an intercept δ_0 and slope δ_1 ,

$$\sigma_G = \delta_0 + \delta_1 |l_I|. \quad (10)$$

Mislocated fixations. A substantial proportion of variability in fixation durations can be attributed to the fixation position relative to the center of an object. During reading, average fixation durations are longest near word centers and decrease towards word edges (Vitu, McConkie, Kerr, & O'Regan, 2001). During visual search, fixation durations decrease with increasing distance to the stimulus element (Trukenbrod & Engbert, 2007). Nuthmann, Engbert, and Kliegl (2005; see also Engbert & Nuthmann, 2008) suggested that the oculomotor system compares intended and realized saccades and immediately initiates a new saccade program when both differ. Such a comparison could be based on an efference copy and might be independent of new visual input. Thus, the initiation of a corrective saccade occurs immediately after the end of a saccade without temporal delay. Corrective saccades have been incorporated into models of eye-movement control during reading and account for fixation duration differences within words (Engbert et al., 2005; Reichle, Warren, & McConnell, 2009).

We calculated the horizontal distance $\Delta_k(t)$ of landing site $k(t)$ at the beginning of fixation n at time t to the center of the intended target stimulus χ_{tar} , i.e.,

$$\Delta_k(t) = |\chi_{tar} - k(t)|. \quad (11)$$

We assume that the oculomotor system is more likely to detect a mislocated fixation with increasing difference between realized and intended saccade. The probability $\eta_n(t)$ to immediately initiate a new saccade program at the beginning of fixation n at time t is a symmetric function around the center of the target stimulus and calculated by a sigmoidal function scaled to values between $0 \leq \eta_n(t) \leq 1$,

$$\eta_k(t) = \frac{\tanh(\nu_1 \Delta_k(t) + \nu_2) + 1}{2}, \quad (12)$$

where ν_1 and ν_2 are two free parameters affecting the point of inflection and slope of the function.

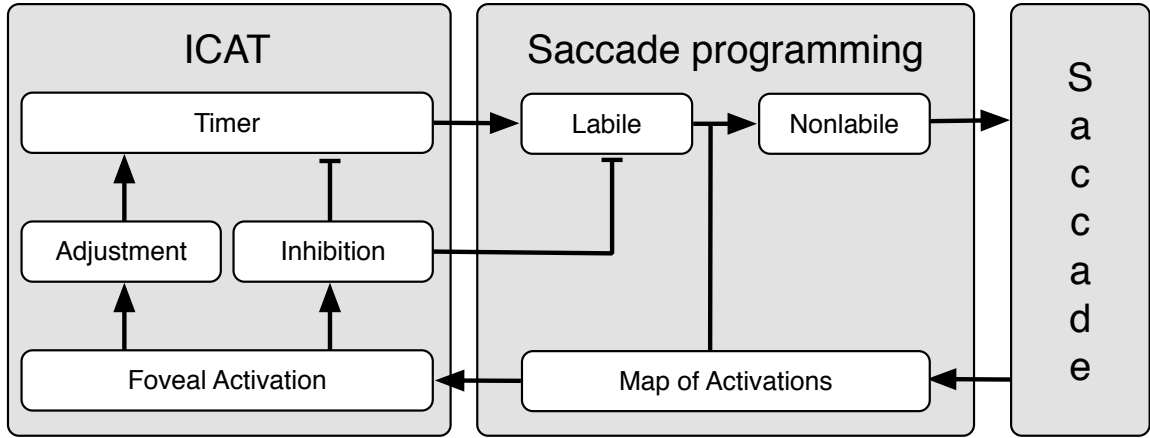


Figure 5. Model overview. The ICAT principles incorporated into a general model of eye-movement control.

Model overview

Figure 5 gives an overview of the full model architecture. Saccade initiation is controlled by the ICAT principles, illustrated in the leftmost part of the figure. Saccades are triggered by an autonomous saccade timer (principle Local I). After a random time interval a new saccade program is initiated, which consists of two stages. During the labile programming stage saccades may still be modified or even canceled. When passing into a non-labile programming stage, a saccade target is selected and saccade execution is inevitable. Saccade targets will be chosen from an activation field defined as a set of activations. Temporal dynamics in the activation field strongly depend on the current fixation position and change after each saccade correspondingly. As stated earlier, foveal processing feeds back to the ICAT model. Thus, foveal activations are used to inhibit the initiation of new saccades (principle Local II) and adjust saccade timing to new processing demands (principle Global).

Specific model assumptions for the scanning task

Saccade initiation intervals and processing. The decision *when* to initiate a new saccade program is generated by the ICAT model as described in the main text. The rate $\omega_j(t)$ of the timer random walk during fixation j is given by the number of states N_t , its average duration T_j , and the strength of foveal inhibition at time t (see Eq. (5) in main text). While we assume that the number of states N_t is constant over time, mean duration T_j varies with fixation history and depends on the expected processing difficulty A_j during fixation j . The expected processing difficulty A_j is estimated from experienced processing difficulty during previous fixations (cf., Eq. (7) in main text). For simplicity, we confine the influence of fixation history to the last symbol, i.e.,

$$A_j = \begin{cases} A_l & \text{if the last processed symbol had a large gap} \\ A_s & \text{if the last processed symbol had a small gap} \end{cases} . \quad (13)$$

Mean duration T_j of a random walk depends on the expected processing difficulty A_j (cf., Eq. (8) in main text). Since we used only two different distractors in our experiment, we decided to estimate mean durations T_l and T_s for each symbol separately, i.e.,

$$T_j = \begin{cases} T_l & \text{for expected difficulty } A_l \\ T_s & \text{for expected difficulty } A_s \end{cases} . \quad (14)$$

For a continuum of stimulus elements with varying target-distractor similarities (or a continuum of word difficulties during reading), a mathematical relation between the maximum of the activation, A_j , and the corresponding mean duration T_j can be estimated (cf., Eq. (7) & (8) in main text). In general, higher expected processing difficulty A_j will cause longer first-passage times of the random walk.

Target selection and mislocated fixations. Since our experiments are one-dimensional scanning tasks, we limited spatial aspects of our model to the horizontal component. In both experiments, saccades aimed at the center of the target symbol, i.e., $l_I = \chi_{tar}$ (see Eq. (8)). Thus, generating a preference to fixate on an object in order to minimize processing time of the fixated stimulus. Because of systematic and oculomotor error actual saccade targets deviate from intended saccade targets. Due to the mislocated fixations mechanism, large deviations immediately initiate a new saccade program at the beginning of a fixation to correct for the observed deviation. The relation between landing site and intended saccade target for both experiments is visualized in Figure 6. When saccades land on the intended target stimulus probability of programming a corrective saccade is minimal. However, with increasing distance to a symbol's center the probability increases until a corrective saccade is almost always initiated when saccades land in the center of two adjacent stimulus elements.

Modeling gaze-contingent displays. In Experiment 2, the activation A_x of a masked stimulus element was limited to the processing difficulty A_s . Since identification of masked stimulus elements was impossible, processing did not enter the second (decreasing) stage when the maximum was reached. Instead, the activation remained at the maximum value, $a_n(t) = A_x$, until the stimulus was fixated by the model. When the fixation of a masked stimulus started, its activation was reset to zero (since parafoveal preprocessing was precluded by the mask), $a_k(t) = 0$, and processing was re-started. The parafoveal build up of activation was necessary to provide saccade targets. Foveal identification, however, was independent of this build up. After saccades away from an item, processing continued as in Experiment 1 when activations had progressed to the second processing stage. Otherwise parafoveal build up started anew.

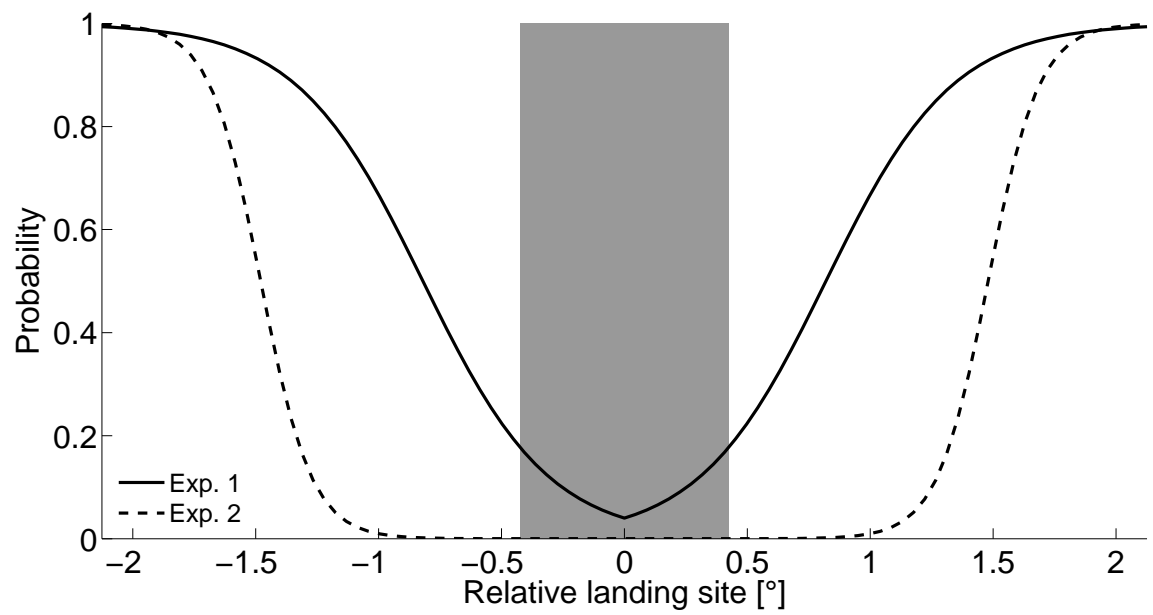


Figure 6. Probability of immediately initiating a new saccade program as a function of the landing site's distance to the target symbol's center. The gray area represents the position and size of the targeted stimulus.

Estimation of model parameters for the full eye movement model

We determined the free model parameters using a *genetic algorithm* approach (Holland, 1992; Mitchell, 1996), which was successfully applied to the SWIFT model (Engbert et al., 2005).⁶ For Experiment 1, we estimated 13 free parameters. Five additional parameters, i.e., average duration of the labile and non-labile saccade programming stages, T_{lab} and T_{nlab} , average duration of a saccade, T_{ex} , number of oculomotor states, N_o , as well as a parameter for target selection, γ , were fixed prior to the estimation process. In Experiment 2 another four parameters were fixed to values estimated in the first experiment: Processing difficulty of easy and difficult stimuli, A_l and A_s , the preprocessing factor f , and the global decay parameter κ . For both experiments we estimated parameters using half of the subjects and assessed the quality of simulations with the second half.

As error metric we computed the weighted deviation of the experimental data (first half) from the simulated data on a number of performance measures. Relative weights are given in brackets. For simulations of Experiment 1 performance of the model was evaluated (i) for durations of the first fixation on a stimulus (3.0E0), (ii) the duration of the n th fixation relative to a change (3.0E0 for absolute values, 1.0E1 for the difference between conditions), (iii) proportion of forward saccades, refixations, and skipings (4.0E4, 4.0E4, 2.0E4), (iv) distribution of first fixations on a stimulus (4.0E5), (v) modulations of fixation durations and refixation rate by fixation position within a stimulus (1.0E3, 2.0E0). In addition, we introduced a penalty for simulations that did not scan the sequence within 27 fixations or within 6.75 s (1.0E2). A list of estimated parameters is presented in Table 3 containing the best fitting set of parameters, mean, and standard error. Additionally, Table 3 informs about the range of possible parameter values submitted to the genetic algorithm.

Simulations of Experiment 2 were evaluated by comparing model simulations with a) mean first-fixation durations on a stimulus (1.5E1), b) distributions of first-fixation durations at relative position 1 (5.0E6), c) proportion of forward saccades (1.0E5), and d) mean fixation durations relative to the symbol center as well as corresponding refixation rates (1.0E0, 5.0E4). Estimated parameters are presented in Table 4.

From the perspective of minimal modeling, we aim at a model with as few parameters as possible. Fortunately, statistical models of oculomotor errors do not require additional free parameters, since all parameters in Equations 9 and 10 can be estimated from experimental data (McConkie et al., 1988). However, four parameters ($l_I, \delta_{SRE}, \delta_0, \delta_1$) have to be estimated separately for forward saccades, forward and backward refixations, skipings, and regressions. Table 5 summarizes parameter combinations for Experiment 1 and Experiment 2, respectively.

Out of the nine fixed parameters in the simulations of the experiments, four parameters were related to oculomotor control and were computed from the experimental data by analyzing the saccadic range effect and variability of landing sites (cf., McConkie et al., 1988). There was no hand-tuning of these parameters, since they are determined by the data.

The remaining five parameters belong to saccade programming and did not vary in the main simulations. These parameters were hand-tuned at an early stage of model

⁶Genetic algorithms do not necessarily find the optimal, best-fitting solution and depend on the error metric used.

Table 3: Model parameters: Experiment 1

Parameter	Symbol	Best	Mean	Error	Min	Max	Reference
Processing parameters							
Activation (Large gap)	A_l	110.41	111.81	2.10	30.0	130.0	Eq. (13)
Activation (Small gap)	A_s	230.11	230.11	< 0.01	30.0	520	Eq. (13)
Visual processing							
Visual span (right)	σ_R	3.47	3.47	< 0.01	1.0	7.0	Eq. (2)
Visual span (left)	σ_L	1.69	1.68	< 0.01	0.0	7.0	Eq. (2)
Global decay	κ	0.26	0.26	< 0.01	0.0	1.0	Eq. (4)
Preprocessing	f	50.33	50.26	0.78	1.0	100.0	Eq. (4)
Saccade timing							
Timer states	N_t	75.00	83.22	5.79	2.0	120.0	Eq. (3) ^b
Duration ^a (Large gap)	T_l	205.82	241.50	0.34	150.0	250.0	Eq. (14)
Duration ^a (Small gap)	T_s	241.55	237.26	0.47	150.0	310.0	Eq. (14)
Foveal inhibition	α	0.19	0.19	< 0.01	0.0	0.5	Eq. (5) ^b
Foveal inhibition	β	3.40	3.40	< 0.01	1.0	10.0	Eq. (5) ^b
Saccade programming							
Oculomotor states	N_o	20.00					Eq. (7)
Duration ^a (Labile)	T_{lab}	125.00					Eq. (7)
Duration ^a (Non-labile)	T_{nlab}	40.00					Eq. (7)
Duration ^a (Execution)	T_{ex}	25.00					Eq. (7)
Target selection weight	γ	0.10					Eq. (5)
Mislocated fixations	ν_1	1.94	2.02	0.17	0.5	5.0	Eq. (12)
Mislocated fixations	ν_2	-0.82	-0.82	< 0.01	-3.0	0.5	Eq. (12)

^aAll durations are presented in ms.

^bEquations from the main text.

development and were kept constant afterwards. We used neurophysiological plausibility when possible (duration of labile and non-labile programming stage, saccade execution). In control simulations, where these parameters were treated as free parameters, we obtained similar estimates, always within the neurophysiologically predicted range.

Regarding variations of visual processing, saccade programming, and oculomotor control parameters in Experiment 1 and 2: We tried to fix as many parameters as possible, however, all critical parameters had to be treated as free parameters to obtain acceptable model fit. In the case of visual processing, we only varied the size of the processing span. A much narrower processing span seems reasonable when processing is limited to the fixated stimulus.

Saccade programming and oculomotor control: The only free parameters of saccade programming that varied were parameters related to mislocated fixations. Differences might be related to the instruction given to subjects. In Experiment 1 subjects were free to move

Table 4: Model parameters: Experiment 2

Parameter	Symbol	Best	Mean	Error	Min	Max	Reference
Processing parameters							
Activation (Large gap)	A_l	110.41					Eq. (13)
Activation (Small gap)	A_s	230.11					Eq. (13)
Visual processing							
Visual span (right)	σ_R	2.15	2.15	< 0.01	0.0	7.0	Eq. (2)
Visual span (left)	σ_L	1.66	1.66	0.01	0.0	7.0	Eq. (2)
Global decay	κ	0.26					Eq. (4)
Preprocessing	f	50.33					Eq. (4)
Saccade timing							
Timer states	N	20.00	20.32	0.32	2.0	120.0	Eq. (3) ^b
Duration ^a (Large gap)	T_l	307.91	306.93	0.49	280.0	360.0	Eq. (14)
Duration ^a (Small gap)	T_s	320.34	320.14	0.91	280.0	390.0	Eq. (14)
Foveal inhibition	α	0.05	0.05	< 0.01	0.0	0.1	Eq. (5) ^b
Foveal inhibition	β	4.35	4.35	0.04	0.0	10.0	Eq. (5) ^b
Saccade programming							
Oculomotor states	N_o	20.00					Eq. (7)
Duration ^a (Labile)	T_{lab}	125.00					Eq. (7)
Duration ^a (Non-labile)	T_{nlab}	40.00					Eq. (7)
Duration ^a (Execution)	T_{ex}	25.00					Eq. (7)
Target selection weight	γ	0.10					Eq. (5)
Mislocated fixations	ν_1	4.81	4.94	0.65	0.5	6.0	Eq. (12)
Mislocated fixations	ν_2	-1.48	-1.49	0.02	-3.0	0.5	Eq. (12)

^aAll durations are presented in ms.^bEquations from the main text.

Table 5: Model parameters for oculomotor control

Experiment	Saccade type	l_I	σ_G	δ_0	δ_1
1: Stepwise change	Forward saccade	4.20	0.25	0.65	0.05
	Forward refixation	1.90	0.25	0.65	0.05
	Backward refixation	1.00	0.25	0.65	0.05
	Regression	5.40	0.00	0.65	0.15
	Skipping	9.00	0.25	0.65	0.05
2: Gaze-contingent	Forward saccade	4.20	0.85	0.45	0.006
	Forward refixation	0.90	0.6	0.45	0.006
	Backward refixation	0.75	0.70	0.45	0.006
	Regression	0.00	0.00	0.45	0.015

their eyes as they wanted, while in Experiment 2 subjects were instructed to make saccades from one item to the next. Furthermore, due to increased fixation durations, model fit was much stronger affected by the IOVP effect in Experiment 2. As mentioned above, oculomotor parameters are given by the experimental data. Saccade targeting of subjects differed between both experiments.

Simulation studies: Target selection & oculomotor control

The main focus of the ICAT model is to provide a framework for the control of fixation durations. Nevertheless, it is important to consider both temporal and spatial dynamics of eye movements. The upcoming section evaluates the performance of the full eye movement model on target selection and oculomotor control related to the fixation position. The effects discussed here are compatible with simulation results of earlier versions of SWIFT (Engbert et al., 2005) and are not generated by the ICAT principles. However, due to the dynamic nature of our model saccade timing modulates the effects generated by other components.

Experiment 1: Stepwise processing change during visual search

Saccade type probabilities. Figure 7 shows the proportion of forward saccades (top panels), skippings (middle panels), and refixations (bottom panels) after the initial fixation of a stimulus. Note, classification of saccade types differs in eye movement research during reading and visual search. Here, refixations refer to all saccades that move the eyes within a symbol n , forward saccades move the eye to the next symbol $n + 1$, and skippings move the eye even further to symbols $\geq n + 2$. Saccades targeting symbols left of the fixated item, i.e., symbol $\leq n - 1$, were classified as regressions.

In the high difficulty condition, participants generate more forward saccades and refixations as well as less skippings than in the low difficulty condition (black solid lines vs. gray solid lines). The same qualitative behavior is produced in our model simulations. The difference between both conditions, however, is less pronounced. When processing demands change (dashed lines), the proportion of forward saccades, skippings, and refixations varies relative to the new stimulus difficulty as early as on the last stimulus before a change (position 0). As in the experimental data, target selection of the model adapts on the last stimulus before a change. Thus, in both the experimental data and the model simulations parafoveal preview is utilized for target selection. The model captures some of the qualitative findings of target selection. However, as can be seen in the correlation plots, systematic deviations from the experimental data are generated. Since the focus of our model is the control of fixation durations, we believe that the spatial behavior is sufficiently reproduced.

Since effects were considerably smaller in the simulations than in the experimental data we compared performance in the two control conditions. For both experiment and simulations we computed ANOVAs with condition (2 factors: high vs. low) and fixation position (5 factors: -1 to 3) as factors. ANOVAs were based on the same number of participants both for the experiment and simulation. While the main effect of condition was present in both data sets for skippings and refixations (all $p < 0.001$), the probability of forward saccades differed only in the experimental data set (experiment: $p < 0.001$, simulation: $p = 0.538$).

Oculomotor control. During visual search, a substantial proportion of variability in oculomotor behavior is related to the fixation position within the fixated stimulus (Trukenbrod & Engbert, 2007). Since our task is a one-dimensional scanning task, we restricted our analysis to the horizontal component. Distributions of fixation positions, mean fixation durations, and refixation probabilities relative to the center of the fixated stimulus element are shown in Figure 8 (upper panels). The spatial extension of the fixated

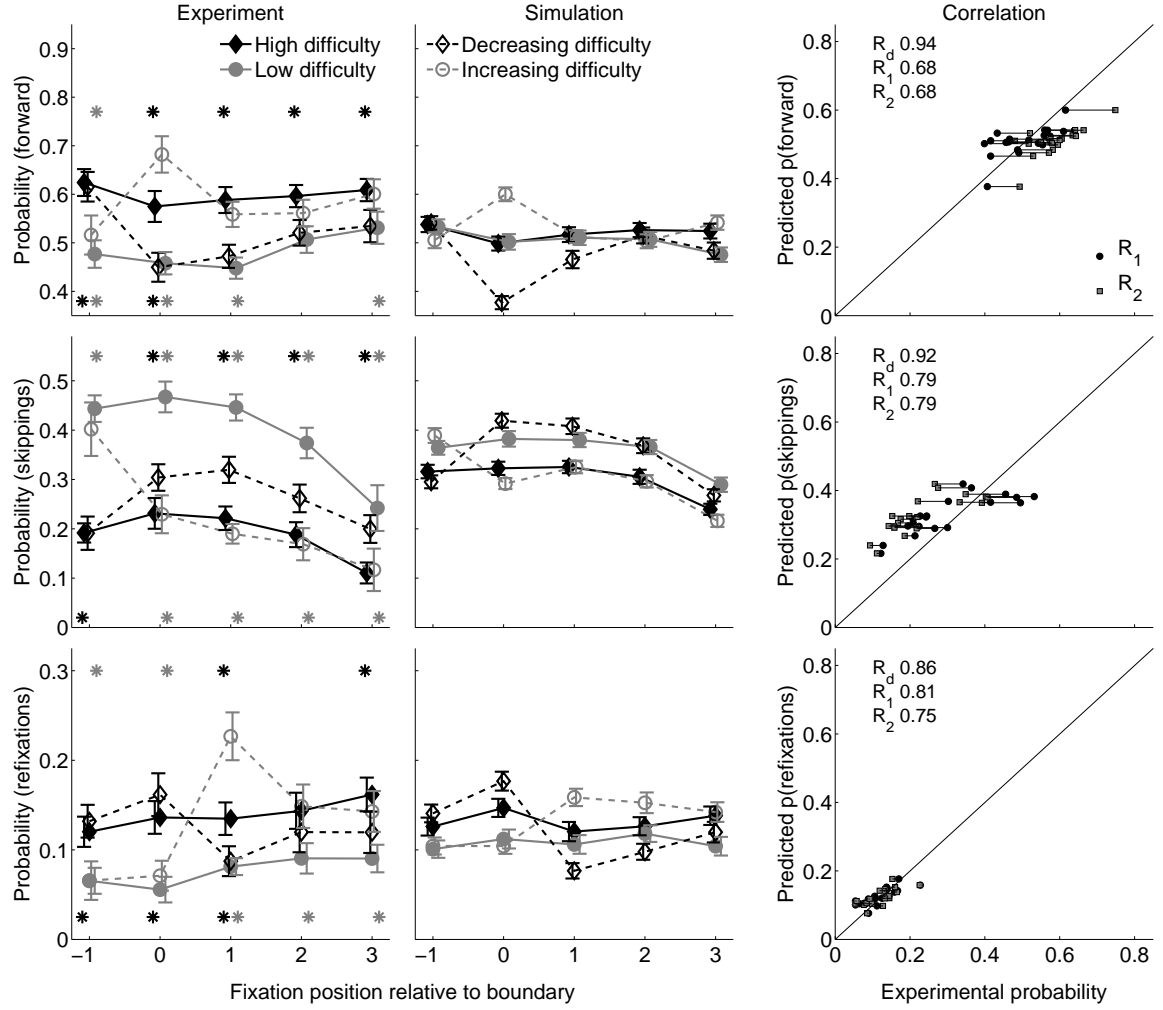


Figure 7. Probability of forward saccades (top panels), skippings (central panels), and refixations (bottom panel) relative to the change in gap size. Left panels: Experimental data; central panels: Simulation panel results. Solid lines represent baseline conditions without a change in gap size. In the remaining conditions gap size changed at position 1 (dashed lines). Trials beginning with a fixation on a stimulus elements with a small gap are plotted in black and trials beginning with a fixation on a large gap are plotted in gray. Error bars indicate confidence intervals based on Cousineau (2005). Asterisks show significant paired-sample t-tests ($p < 0.05$) between experimental conditions (top row: decreasing difficulty; bottom row: increasing difficulty) and baseline conditions (gray asterisks: low difficulty; black asterisks: high difficulty). Right panels: Comparison of simulations with first and second half of the experimental data. R_d gives the correlation between first and second half of the experimental data. R_1 and R_2 indicate correlations between simulated data and first half and second half, respectively.

stimulus is indicated by the gray area in each of the sub-plots. Experimental data indicated by solid lines and simulation results are given by dashed lines. All results were averaged across conditions, different stimulus elements, and participants.

Experimental and simulated landing site distributions are shown in the left panel of Figure 8. First fixations on a stimulus were generally close to its center with some variability around this preferred fixation position. Since saccades aimed at the center of stimulus elements in our model, landing sites are shifted leftward in comparison to the experimental data. Comparing both distributions reveals that a simple mechanism that always targets at the center of a stimulus roughly approximates fixation positions in this task. Nevertheless, a more sophisticated targeting mechanism seems necessary to account for the systematic shift of the landing site distribution.

Next, we inspected fixation durations at different fixation positions (central panel in Fig. 8). Fixation durations decrease towards word edges during reading Vitu et al. (2001; see also Nuthmann et al., 2005; Nuthmann, Engbert, & Kliegl, 2007) or with increasing distance to the center of a stimulus in visual search (Trukenbrod & Engbert, 2007). The same relation can be observed in both our experiment and model. Fixation durations peak close to the center of a stimulus and decrease with increasing distance to the symbol. This qualitative behavior is predicted by the hypothesis that mislocated fixations are more frequently placed at word edges, where the triggering of error-correcting saccade induce a decrease in fixation durations. Fixation durations reach an asymptote of about 150–175 ms as a function of the distance from the center of the fixated symbol. The asymptotic value of duration corresponds to the minimum programming time of a saccade and suggests that the decision to initiate a new saccade at this location is made at the beginning of a fixation and is independent of the visual input as predicted by the efference copy assumption discussed above.

Finally, we investigated the probability of refixating a stimulus depending on the fixation position within an object (McConkie et al., 1989; Trukenbrod & Engbert, 2007). Refixation rate is asymmetrically affected by relative fixation position. The probability to refixate a stimulus is highest when fixations are left of the stimulus and decreases towards the symbol. After reaching a minimum rate close to the center of the stimulus, refixation rate right of a stimulus increases moderately. Model simulations reveal a qualitatively similar trend. However, simulations show a much steeper decline from the left to the right and no increase to the right of the center. Compared to other oculomotor effects, the probability of refixations is rather poorly captured. This is also evident in the correlation plot revealing systematic deviations for first and second half of the experimental data.

Experiment 2: Gaze-contingent display presentation

Saccade type probabilities. As for the first experiment, we examined target selection of our model. Probabilities to move from one stimulus to the next after its first fixation are plotted in Figure 9. Across positions we observe differences between conditions. These differences, however, are smaller and less reliable compared to the differences found in Experiment 1. In baseline conditions, forward saccades are more likely when fixating a simple stimulus (black solid line vs. gray solid line). For increasing processing demands, rate of forward saccades immediately drops after fixating the first difficult stimulus (gray dashed line). As observed in the pattern of fixation durations, this reduction is larger

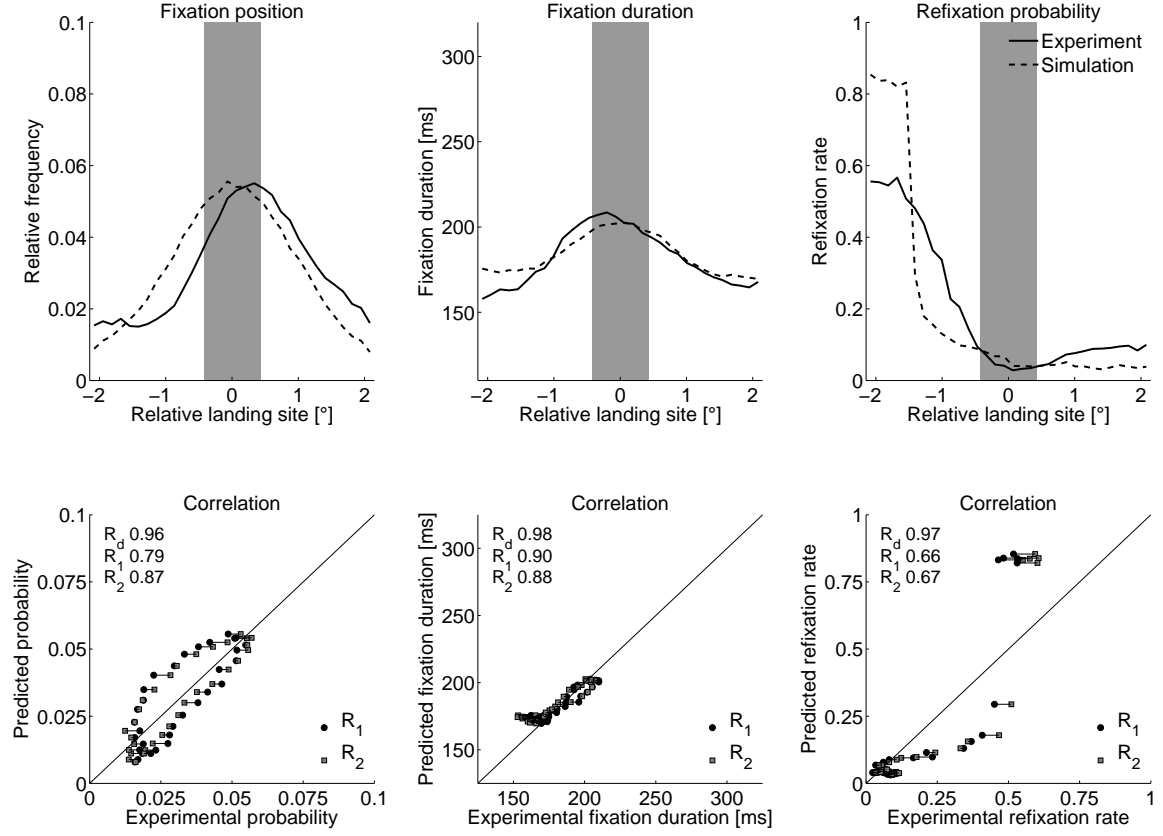


Figure 8. Oculomotor control: Effects of fixation position. Upper panels: In each plot, the horizontal axis represents the fixation position relative to the center of the fixated stimulus element. Solid lines indicate observed experimental data, simulated data are plotted with dashed lines. Left panel: Distribution of fixation positions; central panel: Fixation durations; right panel: Refixation probability. Lower panels: Comparison of simulations with first and second half of the experimental data. R_d gives the correlation between first and second half of the experimental data. R_1 and R_2 indicate correlations between simulated data and first half and second half, respectively.

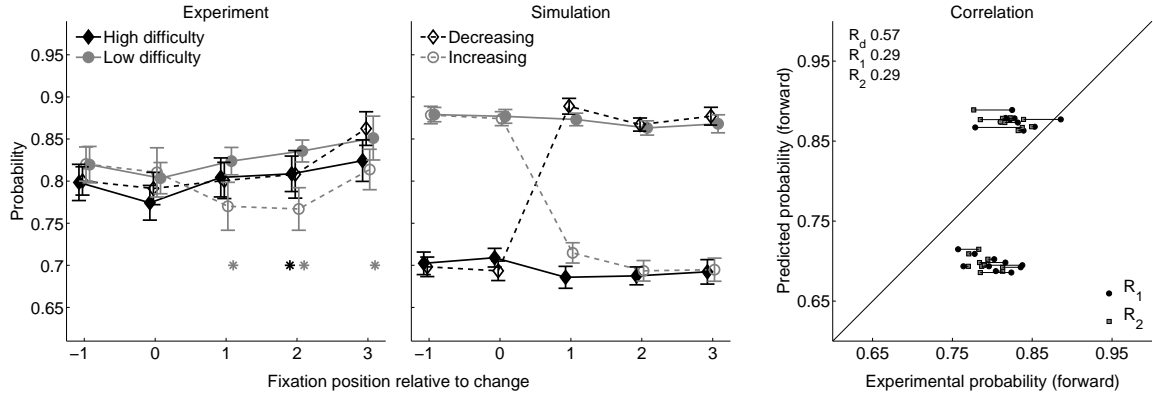


Figure 9. Probability of forward saccades relative to a change in gap size. Left panel: Experimental data; central panel: Simulation results. Solid lines represent baseline conditions without a change in gap size. In other conditions gap size changed at position 1 (dashed lines). Trials starting with stimulus elements with a small gap are plotted in black and trials starting with a large gap are plotted in gray. Error bars indicate confidence intervals based on Cousineau (2005). Asterisks show significant paired-sample t-tests ($p < 0.05$) between experimental conditions (top row: decreasing difficulty; bottom row: increasing difficulty) and baseline conditions (gray asterisks: low difficulty; black asterisks: high difficulty). Right panel: Comparison of simulations with first and second half of the experimental data. R_d gives the correlation between first and second half of the experimental data. R_1 and R_2 indicate correlations between simulated data and first half and second half, respectively.

than expected by the baseline condition revealing a tendency to overcompensate for the increased processing demands. During target selection, however, this overcompensation seems to endure across multiple stimulus elements. In contrast, for decreasing processing demands (black dashed line), rate of forward saccades remains low for up to two stimuli after a change. Interestingly, neither the fixation duration nor the rate of forward saccades reflects decreased processing demands at position 1.

Simulation results are plotted in the central panel of Figure 9. As observed during the experiment, rate of forward saccades is lower on difficult stimuli (black solid line vs. gray solid line). When processing demands change, simulations show an immediate adjustment towards the new baseline condition. Hence, target selection in its current implementation is strongly based on moment-to-moment processing, but over- and underestimation of saccade probabilities confirms our conclusions from Experiment 1 that target selection is currently too simplistic to capture all details of saccade targeting.

Finally, as for Experiment 1 we computed ANOVAs based on the same number of subjects to get an estimate of reliability of the difference in forward saccade observed in the two control conditions. The probability of forward saccades differed in both experiment ($p < 0.05$) and simulation ($p < 0.001$).

Oculomotor control. Finally, we also investigated oculomotor behavior related to the fixation position within an object. Horizontal landing site distributions are shown in the

left panel of Figure 10. In general, initial landing positions are close to the center of a symbol with a narrow distribution around the fixated stimulus element. Model simulations nicely reproduce average landing site as well as its variability.

Fixation duration modulations relative to the fixated stimulus are shown in the central panels of Figure 10. As expected, fixation durations decrease towards adjacent stimulus elements. Compared to the first experiment, absolute effect size is much larger since fixation durations at the center rise from about 220 ms to approximately 300 ms in Experiment 2, while fixation durations beside the stimulus remain at around 150 ms in both experiments. Overall, the strong effect is replicated by our simulations. The current implementation, however, generates a symmetrical modulation leading to a weaker effect to the left of a stimulus and a stronger effect to the right of a stimulus.

In a final analysis we compared refixation rate within a stimulus. As observed in the previous experiment, refixation rate is asymmetrically affected by landing site. Refixation rate is highest left of the stimulus, decreases towards the center, and rises towards the right. Model simulations show the same qualitative behavior, but give just a rough approximation of the observed refixation rates.

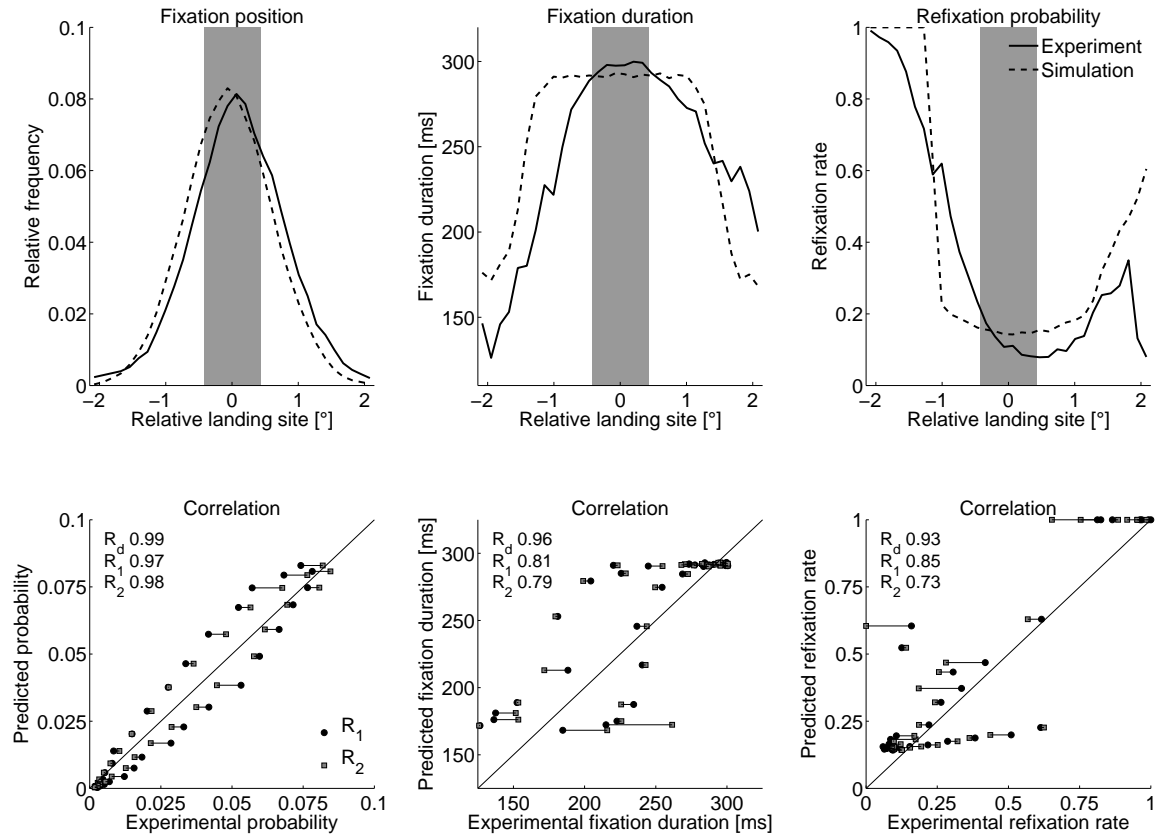


Figure 10. Oculomotor control: Effects of fixation position. Upper panels: In all plots, the x-axis represents the horizontal fixation position relative to the center of the fixated stimulus element. Solid lines show observed experimental data, simulated data are plotted with dashed lines. Left panel: Distribution of fixation positions; central panel: Fixation durations; right panel: Refixation probability. Lower panels: Comparison of simulations with first and second half of the experimental data. R_d gives the correlation between first and second half of the experimental data. R_1 and R_2 indicate correlations between simulated data and first half and second half, respectively.

Experimental Details

Experiment 1: Stepwise change in processing demands

Participants. We tested 32 participants (23 female, 9 male), all students at the University of Potsdam, with an average age of 23 years ranging from 19 to 39 years. All subjects received study credits or were paid 9€ and reported normal or corrected-to-normal vision.

Task, stimuli, and procedure. Participants were instructed to scan sequences for a target symbol from left-to-right. Target presence and absence had to be indicated by making a saccade to the upper or lower right corner of the screen with response mapping being counterbalanced across participants. Responses were evaluated and errors caused a short beep at the end of a trial. We tested four conditions (Fig. 10 in main text). Stimulus elements in the baseline conditions had constant difficulty, while processing demands increased/decreased in the other conditions. Search arrays consisted of eleven horizontally arranged stimuli with a center-to-center distance of 4.32° . Changes occurred on the fifth to eighth stimulus and were equally likely at all four positions. There was only one change in trials with varying processing demands.

Targets were black rings with an absolute size of $.86^\circ$ and a line-width of $.23^\circ$ when presented in front of the participant at the center of the screen. We manipulated processing demands by varying target-distractor similarity with “easy” distractors having a larger gap than “difficult” distractors ($.14^\circ$ vs. $.05^\circ$). Gaps were located in one of four cardinal positions (top, bottom, left, right) and all stimuli were presented on a light gray background.

Each trial started with the presentation of a small black fixation cross (each line: $.64^\circ \times .18^\circ$). Trials continued if both eyes remained within a fixation area centered around the cross ($1.77^\circ \times 1.77^\circ$) for 200 ms. After successful fixation the fixation cross disappeared and the search array was presented. The leftmost stimulus of the array was centered on top of the fixation cross. After scanning the sequence subjects indicated target presence/absence. The next trial started after response evaluation. Overall participants searched 256 trials. Targets were present in 25% of trials and the order of trials was randomized. Eye movements were recalibrated every fifteenth trial or when a fixation check failed three times in succession.

Apparatus. Stimulus presentation was controlled by an Apple Power Macintosh G4 computer and presented on a 22-in. Iiyama Vision Master Pro 514 CRT (resolution: 1024×768 , refresh rate: 100 Hz). We recorded eye movements using the video-based Eyelink-II system (SR Research, Osgoode, ON, Canada) with a sampling rate of 500 Hz and used a chin rest to reduce head movements. Stimulus presentation and response collection were implemented in MATLAB (The MathWorks, Natick, MA, USA) using the Psychophysics Toolbox (PTB2; Brainard, 1997; Pelli, 1997) as well as the Eyelink Toolbox (Cornelissen, Peters, & Palmer, 2002).

Data preprocessing. We limited our analyses to target-absent trials. Saccades were detected using a velocity-based algorithm developed by Engbert and Kliegl (2003; improved by Mergenthaler and Engbert, 2006). Saccades were detected whenever both eyes exceeded a velocity threshold in 2D velocity space (5 SD) for at least 6 successive data points (12 ms)

with a minimum amplitude of 0.29° ($1/3$ symbol size). For each fixation we computed a mean fixation position and assigned it to the closest symbol. Trials with blinks or fixations outside the monitor were excluded from further analyses as well as fixations on the first and last stimulus of the array.

Experiment 2: Gaze contingent display presentation

Participants. 30 persons (27 female, 3 male) participated in the experiment. Subjects were either pupils at a local school in Potsdam or students of the University of Potsdam. All received course credits or were paid 9€. On average participants were 21 years ranging from 15 to 34 years. All participants had normal or corrected-to-normal vision.

Task and stimuli. In the second experiment we limited processing to the fixated stimulus by presenting stimulus elements gaze-contingent. While the fixated stimulus was visible as in the previous experiment, other stimuli were masked by quadratic Xs with a side length of $.86^\circ$ and a line width of $.18^\circ$. Except for the gaze-contingent manipulation we presented the same sequences as in Experiment 1. All specifications remained unchanged.

Participants were explicitly told to fixate stimuli from left-to-right without skipping single elements. Eye-position was continuously monitored and assigned to the closest symbol. As soon as the eyes moved to another stimulus an X masked the previously fixated stimulus and the fixated stimulus appeared on the screen. Participants scanned the sequence until they had inspected all symbols and responded whether they had found the target by making an eye-movement to the upper/lower right corner of the screen. Response mapping was counterbalanced across participants.

Apparatus. The same technical setup was used as in Experiment 1.

Data preprocessing. Data preprocessing was the same as in Experiment 1. To ensure that participants acted in accordance with the instruction and in order to reduce noise due to poorly calibrated trials, we excluded trials with regressions, i.e., saccades to previously inspected elements, as well as trials where participant's eyes skipped single elements.

References

- Amari, S. (1977). Dynamics of pattern formation in lateral-inhibition type neural fields. *Biological Cybernetics*, 27, 77–87.
- Becker, W., & Jürgens, R. (1979). An analysis of the saccadic system by means of double step stimuli. *Vision Research*, 19, 967–983.
- Brainard, D. H. (1997). The Psychophysics Toolbox. *Spatial Vision*, 10, 443–446.
- Caspi, A., Beutter, B. R., & Eckstein, M. P. (2004). The time course of visual information accrual guiding eye movement decisions. *Proceedings of the National Academy of Sciences USA*, 101(35), 13086–13090.
- Cornelissen, F. W., Peters, E., & Palmer, J. (2002). The Eyelink Toolbox: Eye tracking with MATLAB and the Psychophysics Toolbox. *Behavior Research Methods, Instruments & Computers*, 34, 613–617.
- Cousineau, D. (2005). Confidence intervals in within-subject designs: A simpler solution to Loftus and Masson's method. *Tutorial in Quantitative Methods for Psychology*, 1(1), 42–45.
- Drieghe, D., Rayner, K., & Pollatsek, A. (2008). Mislocated fixations can account for parafoveal-on-foveal effects in eye movements during reading. *The Quarterly Journal of Experimental Psychology*, 61(8), 1239–1249.

- Engbert, R., & Kliegl, R. (2011). Parallel graded attention models of reading. In S. P. Livsedge, I. D. Gilchrist, & S. Everling (Eds.), *The Oxford Handbook of Eye Movements* (pp. 787–800). Oxford, UK: Oxford University Press.
- Engbert, R., & Krügel, A. (2010). Readers use bayesian estimation for eye movement control. *Psychological Science*, 21(3), 366–371.
- Engbert, R., Longtin, A., & Kliegl, R. (2002). A dynamical model of saccade generation in reading based on spatially distributed lexical processing. *Vision Research*, 42, 621–636.
- Engbert, R., & Nuthmann, A. (2008). Self-consistent estimation of mislocated fixations during reading. *PLoS ONE*, 3(2), e1534.
- Engbert, R., Nuthmann, A., Richter, E. M., & Kliegl, R. (2005). SWIFT: A dynamical model of saccade generation during reading. *Psychological Review*, 112, 777–813.
- Erlhagen, W., & Schöner, G. (2002). Dynamic field theory of movement preparation. *Psychological Review*, 109, 545–572.
- Foxe, J. J., & Simpson, G. V. (2002). Flow of activation from V1 to frontal cortex in humans. *Experimental Brain Research*, 142(1), 139–150.
- Gillespie, D. T. (1978). Monte Carlo simulation of random walks with residence time dependent transition probability rates. *Journal of Computational Physics*, 28, 395–407.
- Holland, J. H. (1992). *Adaptation in natural and artificial systems*. Cambridge: MIT Press.
- Kapoula, Z. (1985). Evidence for a range effect in the saccadic system. *Vision Research*, 25(8), 1155–1157.
- Koch, C., & Ullman, S. (1985). Shifts in visual attention: Towards the underlying circuitry. *Human Neurobiology*, 4, 219–222.
- Lamme, V. A. F., & Roelfsema, P. R. (2000). The distinct modes of vision offered by feedforward and recurrent processing. *Trends in Neurosciences*, 23(11), 571–579.
- Martin, E. (1974). Saccadic suppression: A review and an analysis. *Psychological Bulletin*, 81(12), 899–917.
- McConkie, G. W., Kerr, P. W., Reddix, M. D., & Zola, D. (1988). Eye movement control during reading: I. The location of initial eye fixations on words. *Vision Research*, 28, 1107–1118.
- McConkie, G. W., Kerr, P. W., Reddix, M. s., Zola, D., & Jacobs, A. M. (1989). Eye movement control during reading: II. Frequency of refixating a word. *Perception & Psychophysics*, 46, 245–253.
- McConkie, G. W., & Rayner, K. (1975). The span of the effective stimulus during a fixation in reading. *Perception & Psychophysics*, 17, 578–586.
- McConkie, G. W., & Rayner, K. (1976). Asymmetry of the perceptual span in reading. *Bulletin of the Psychonomic Society*, 8, 365–368.
- McPeck, R. M., & Keller, E. L. (2002). Superior colliculus activity related to concurrent processing of saccade goals in a visual search task. *Journal of Neurophysiology*, 87(4), 1805–1815.
- McPeck, R. M., Skavenski, A. A., & Nakayama, K. (2000). Concurrent processing of saccades in visual search. *Vision Research*, 40, 2499–2516.
- Mitchell, M. (1996). *An introduction to genetic algorithms*. Cambridge: MIT Press.
- Nuthmann, A., Engbert, R., & Kliegl, R. (2005). Mislocated fixations during reading and the inverted optimal viewing position effect. *Vision Research*, 45, 2201–2217.
- Nuthmann, A., Engbert, R., & Kliegl, R. (2007). The IOVP effect in mindless reading: Experiment and modeling. *Vision Research*, 47(7), 990–1002.
- Pelli, D. G. (1997). The videotoolbox software for visual psychophysics: Transforming numbers into movies. *Spatial Vision*, 10, 437–442.
- Pollatsek, A., Bolozy, S., Well, A. D., & Rayner, K. (1981). Asymmetries in the perceptual span for Israeli readers. *Brain & Language*, 14, 174–180.
- Poulton, E. C. (1981). Human manual control. In V. B. Brooks (Ed.), *Handbook of physiology. Vol. II. Motor control: Section 1. The nervous system* (pp. 1337–1389). Bethesda, MD: American Physiological Society.

- Rayner, K. (1975). The perceptual span and peripheral cues in reading. *Cognitive Psychology*, 7, 75–81.
- Rayner, K., & Bertera, J. H. (1979). Reading without a fovea. *Science*, 206, 468–469.
- Rayner, K., Liversedge, S. P., White, S. J., & Vergilino-Perez, D. (2003). Reading disappearing text: Cognitive control of eye movements. *Psychological Science*, 14(4), 385–388.
- Rayner, K., Pollatsek, A., & Reichle, E. D. (2003). Eye movements in reading: Models and data. *Behavioral & Brain Sciences*, 26(4), 507–526.
- Rayner, K., Yang, J., Castelhana, M. S., & Liversedge, S. P. (2011). Eye movements of older and younger readers when reading disappearing text. *Psychology & Aging*, 26(1), 214–223.
- Reichle, E. D., Warren, T., & McConnell, K. (2009). Using E-Z Reader to model the effects of higher level language processing on eye movements during reading. *Psychonomic Bulletin & Review*, 16(1), 1–21.
- Reingold, E. M., Reichle, E. D., Glaholt, M. G., & Sheridan, H. (2012). Direct lexical control of eye movements in reading: Evidence from a survival analysis of fixation durations. *Cognitive Psychology*, 65(2), 177–206.
- Reingold, E. M., Yang, J., & Rayner, K. (2010). The time course of word frequency and case alternation effects on fixation times in reading: Evidence for lexical control of eye movements. *Journal of Experimental Psychology: Human Perception & Performance*, 36(6), 1677–1683.
- Staub, A. (2011). The effect of lexical predictability on distributions of eye fixation durations. *Psychonomic Bulletin & Review*, 18(6), 371–376.
- Staub, A., White, S. J., Drieghe, D., Hollway, E. C., & Rayner, K. (2010). Distributional effects of word frequency on eye fixation durations. *Journal of Experimental Psychology: Human Perception & Performance*, 36(5), 1280–1293.
- Trukenbrod, H. A., & Engbert, R. (2007). Oculomotor control in a sequential search task. *Vision Research*, 47, 2426–2443.
- Vitu, F., McConkie, G. W., Kerr, P., & O'Regan, J. K. (2001). Fixation location effects on fixation durations during reading: An inverted optimal viewing position effect. *Vision Research*, 41, 3513–3533.
- White, S. J. (2008). Eye movement control during reading: Effects of word frequency and orthographic familiarity. *Journal of Experimental Psychology: Human Perception & Performance*, 34(1), 205–223.
- Yang, S.-N., & McConkie, G. W. (2001). Eye movements during reading: A theory of saccade initiation times. *Vision Research*, 41, 3567–3585.